Physics and Materials Chemistry, 2015, Vol. 3, No. 2, 18-24
Available online at http://pubs.sciepub.com/pmc/3/2/1

DOI:10.12691/pmc-3-2-1

In-situ Synthesis of PVA/HgS Nanocomposite Films and Tuning Optical Properties

Omed Gh. Abdullah[1,*], Yahya A.K. Salman[2], Salwan A. Saleem[2]

[1]Department of Physics, Faculty of Science and Science Education, School of Science, University of Sulaimani, Kurdistan Region, Iraq
[2] Department of Physics, College of Science, University of Mosul, Iraq
*Corresponding author: omed.abdullah@univsul.edu.iq

Abstract Polymer based nanocomposite films of polyvinyl alcohol (PVA) doped with mercury sulfide (HgS) were prepared via in-situ chemical reduction and the solution cast methods, with different HgS concentrations, in order to study the effect of HgS content on optical properties of PVA. The nanocomposites films were characterized using FTIR, XRD, and SEM. The UV-Visible absorption spectra in the wavelength range (190–1100) nm were analyzed in terms of absorption formula for non-crystalline materials. The band gap and the fundamental optical constants of the prepared samples have been investigated and showed a clear dependence on the HgS concentration. The observed value of band gap for pure polyvinyl alcohol is about 6.27 eV and decreases to a value 4.88 eV for the film of 0.04M HgS content. The refractive index and consequently the related dispersion parameters of PVA and PVA/HgS nanocomposite versus HgS content have been determined and explained using Wemple-DiDomenico single oscillator model.

Keywords: *polymer nanocomposite, mercury sulfide, optical band gap, complex dielectric constant*

Cite This Article: Omed Gh. Abdullah, Yahya A.K. Salman, and Salwan A. Saleem, "In-situ Synthesis of PVA/HgS Nanocomposite Films and Tuning Optical Properties." *Physics and Materials Chemistry*, vol. 3, no. 2 (2015): 18-24. doi: 10.12691/pmc-3-2-1.

1. Introduction

Development of polymer nanocomposites is a fast growing field owing to the exceptional properties from such materials at low filler concentration [1]. The incorporation of the semiconductor nanoparticles into transparent polar polymers matrix can induce significant changes in the ultimate properties of polymers and improve their properties [2,3]. The characteristics of these composite films can be manipulated by controlling the type [4], size [5] and shape of the nanoparticles [6], and the method used to prepare the nanocomposite [7].

The optical properties of polymer nanocomposite have attracted much attention in view of their applications in photonic devices with remarkable reflection, antireflection, and polarization properties [8]. The optical properties of polymers can be suitably modified by the addition of nanoparticles depending on their reactivity with the host matrix [9]. Achieving a deeper insight into their properties is essential not only for scientific knowledge but also for modern and advanced technological applications [10]. Understanding the physical and chemical nature of the nanocomposites structure helps greatly to interpret the conduction mechanism taking place in these types of materials.

Mercury sulfide is one of the most important II-VI semiconductor having excellent optoelectric properties and is widely used in many fields such as ultrasonic transducers, photoelectric conversion devices and infrared sensors [11,12,13]. Because of the toxicity and difficulty in synthesis of mercury sulfide, there are very small reports on synthesis and characteristics of mercury sulfide nanocrystals [14]. Polymers such as Polystyrene [15,16], Polyacrylamide [17,18], Chitosan [19], and Poly(methyl methacrylate) [20] have been extensively utilized for the fabrication of HgS nanocrystals based on polymer matrix.

In the present study, films of polymer based nanocomposites with low HgS concentration were prepared using in-situ chemical reduction of mercury nitrate ($Hg(NO_3)_2$) and sodium sulfide (Na_2S) in aqueous solutions of PVA as capping for different molar content of $Hg(NO_3)_2$ and Na_2S, for the purpose enhance the optical characterization of PVA matrix. The quantitative measurements of optical parameters may help in tailoring and modeling the properties of the films for their use in optical and optoelectronic components and devices.

2. Experimental work

2.1. Nanocomposites Films Preparation

Solution casting method and in situ chemical reduction technique were used to prepare PVA/HgS nanocomposite films. In the present system 2 g of Polyvinyl alcohol (PVA) (98-99% hydrolyzed, low molecular weight) supplied by Alfa Aesar, was dissolved in 30 mL distilled water. The solution was then stirred continuously for one hour at 90 °C until highly homogeneous and the clean viscous polymer solution was formed. Mercury nitrate ($Hg(NO_3)_2$) as Hg^{+2} source and Sodium sulfide (Na_2S) as S^{-2} source, were dissolved in the 5 mL distilled water separately with

different molar concentrations (0, 0.01, 0.02, 0.03 and 0.04) M at ambient temperature.

Then the two solutions with ration 1:1, were added dropwise to the homogeneous aqueous solution of PVA at 40^{o}C under stirring, resulting in the change of color of the solution from colorless to dark red, which indicated that the formation of HgS nanoparticle had begun. For maximum dispersion, the mixture was further stirred continuously for (15 minutes) without heating until the mixture reached a homogeneous viscous molten state. Then the solution was sonicated at 50% amplitude for 1 sec on and 2 sec off for total time 3 minutes.

The homogeneous mixture solutions were cast in a plastic Petri dish with diameter of 8.2 cm in average, and the solvent was allowed to evaporate completely in the open air at temperature (~35°C) and under atmospheric pressure for a week for nanocomposite films to form. The dried films were peeled off and transferred into desiccators for continuous drying. The chemical reaction for the HgS formation is given by:

$$Hg(NO_3)_2(aq) + Na_2S(aq) = HgS(s) + 2NaNO_3(aq)$$

The prepared films have a uniform thickness of (0.04, 0.038, 0.035, 0.035, and 0.037) mm for HgS concentration (0, 0.01, 0.02,0.03 and 0.04) respectively.

2.2. Characterization Techniques

The Fourier transform infrared (FTIR) spectra of the nanocomposites samples were analyzed in the range (400-4000) cm^{-1} using a Perkin Elmer in the transmission mode at a resolution of 1.0 cm^{-1}. The X-ray diffraction (XRD) patterns of the pure PVA film and the PVA/HgS polymer nanocomposite films were recorded using X-ray diffractometer (XPERT-PRO) equipped with monochromatized Cu Kα (λ = 0.154 nm) radiation, and in the 2θ range (10°-70°) to report the information about their structure.

For scanning electron microscopy (SEM), the composites samples were fixed on a very thin transparent glue tape, which was placed on an aluminium stub of 15 mm diameter. The aluminium stub with the sample was then kept in a chamber at very low pressure (10^{-3} bar), where the entire plastic foil containing the sample was sputtered with gold for 5 min using an Emitech (K550X) coater. The gold-coated specimens were then observed on a CamScan 3200 SEM operating at an accelerating voltage of 25 KV, to investigate the morphological appearance of the samples.

The absorption spectra (A) of the prepared films were collected at room temperature in the wavelength range (190-1100) nm, using a double-beam Perkin Elmer (Lambda-25) UV-Vis-NIR spectrophotometer.

3. Results and Discussion

3.1. FTIR Spectroscopic Analysis

The Fourier transform infrared spectra FTIR for pure PVA, and PVA/HgS nanocomposite of 0.04 morality concentration of HgS are presented in Figure 1. The transmittance spectra exhibit the main characteristic of pure PVA, which are stretching and bending vibrations of O-H, C-O, C-C, and C-H groups [21,22]. A broad and strong band centered at 3340 cm^{-1} arises from O-H stretching vibration of hydroxyl groups [23]. The observed peak of -OH group of PVA is shifted in PVA/HgS nanocomposite sample to lower wave number, which indicate the electrostatic interaction between -OH group and HgS nanoparticles [22]. In the FTIR spectrum of PVA/HgS nanocomposite showed a decrease in the intensity of all the bands indicating the charge-transfer complex between PVA molecule chains and HgS nanoparticles [24].

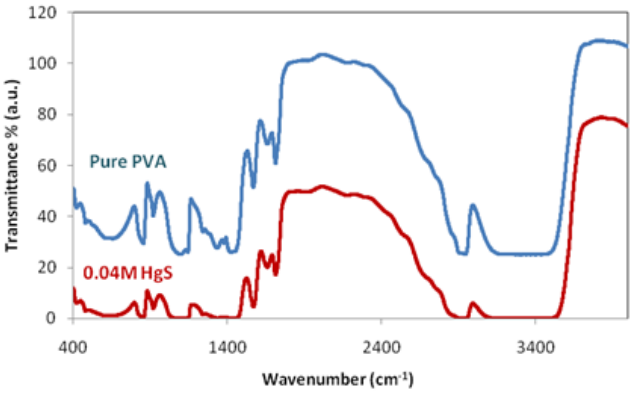

Figure 1. FTIR spectra of pure PVA, and PVA/0.04M HgS nanocomposite films

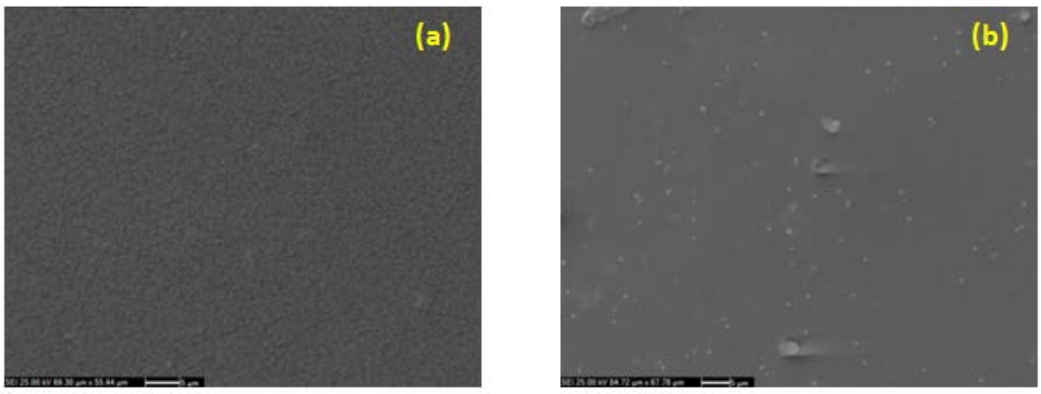

Figure 2. SEM images of PVA/HgS films with (a) 0.01M HgS, (b) 0.04M HgS

3.2. Scanning Electron Microscopy (SEM) Analysis

Figure 2 shows an example of the scanning electron microscopy (SEM) images of PVA/HgS polymer nanocomposite samples with 0.01M and 0.04M, HgS

concentrations. The white spots indicate HgS that shows almost homogeneous dispersion with some aggregation. The shape of HgS particles were roughly spherical.

3.3. X-ray Diffraction (XRD) Analysis

The formation of PVA\HgS nanocomposite was also confirmed using XRD analysis. Figure 3 depicts the compaction of XRD patterns for pure PVA film, PVA/HgS nanocomposite film with 0.04 molar concentrations of HgS, and single hexagonal phase of HgS. The first broad peak appears at $2\theta \approx 19.26^{\circ}$ correspond to the PVA semi-crystalline phase [25]. The semi-crystalline nature of PVA results from the strong intermolecular interaction between PVA chains through the intermolecular hydrogen bonding. The observed small intensity diffraction peaks at scattering angle $2\theta = 26.35^{\circ}$, 27.33°, 30.95°, 43.27°, 45.37°, and 54.07° are corresponding to reflections from (101), (003), (012), (110), (104) and (202) crystal planes, confirmed the formation of the HgS nanoparticles in a PVA matrix. The intensities and positions of these peaks are in agreement with the literature (JCPDS card no. 06-0256) that correspond to the hexagonal phase of HgS (cinnabar) [26,27] (as shown in Figure 3-a). Moreover, no any impurities are detected in the XRD pattern, indicating the high purity of the product. The crystallite sizes of HgS nanoparticles have been determined using Debye-Scherrer formula [28]. The average crystalline sizes of HgS nanoparticles for main peak with $2\theta = 30.95^{\circ}$ were estimated. The average crystallite size was in the range of (13.28 to 16.23) nm.

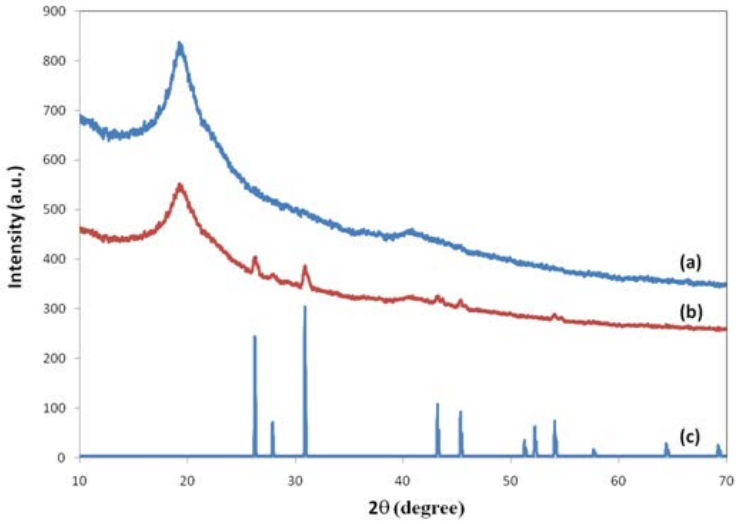

Figure 3. The X-ray diffractogram of (a) pure PVA, (b) 0.04 M HgS nanocomposite and (c) hexagonal phase of HgS

3.4. Optical Parameters

One of the most direct and perhaps the simplest method of investigating the band structure of materials is studying their absorption spectra [29]. The abrupt increase in absorption, known as the fundamental absorption edge, which can be used to determine the band gap and the type of transition [30,31]. Absorption is expressed in terms of the coefficient $\alpha(v)$, which is defined as the relative decrease rate in light intensity. $\alpha(v)$ can be calculated from the optical absorbance spectra A using the Beer Lambert's formula [30,32]:

$$\alpha(v) = \frac{1}{d}\log\left(\frac{I_o}{I}\right) = \frac{2.303}{d}A \qquad (1)$$

where d is the sample thickness; I_o and I are the incident and transmitted intensities, respectively [33]. The variation of the refractive index (n) as a function of wavelength can be obtained from

$$n = \left(\frac{1+R}{1-R}\right) + \sqrt{\frac{4R}{(1-R)^2} - k^2} \qquad (2)$$

where R is reflectance, and k is the extinction coefficient, which is related to the absorption coefficient $\alpha(v)$ and wavelength λ by [34]:

$$k = \frac{\alpha\lambda}{4\pi}. \qquad (3)$$

The UV-Visible absorption spectrum of PVA/HgS nanocomposite films at different HgS concentration of (0, 0.01, 0.02, 0.03, and 0.04) M is shown in Figure 4. It can be seen clearly that the absorption decreases rapidly with increasing wavelength up to 400 nm. Another observation about these absorption spectra is that after adding HgS nanoparticls in PVA polymer matrix, the intensity of absorption spectra continuously increasing with increasing concentration of the dopant.

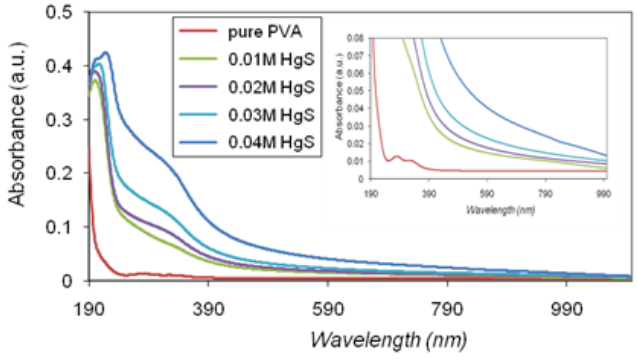

Figure 4. Absorption spectra for PVA/HgS composites

Figure 5 shows the variation of the refractive index (n) of the prepared PVA/HgS nanocomposite films with wavelength, calculated from Eqs. (2) and (3), which relate the refractive index (n) with the absorption coefficient (α) and the extinction coefficient (k). The figure shows that the refractive index decrease with an increase in the wavelength of the incident photon and tends to be constant at high wavelengths as shown in Figure 5.

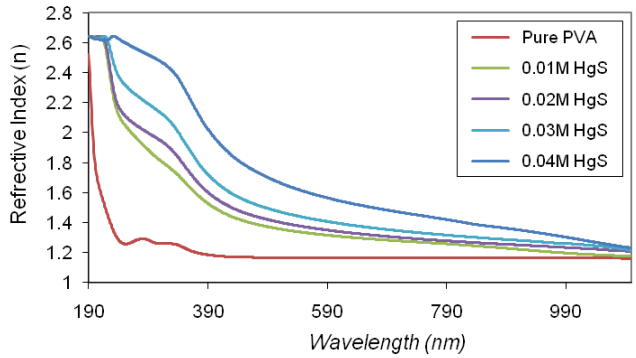

Figure 5. Refractive index versus wavelength for pure PVA and PVA/HgS nanocomposites films

It has been also observed that refractive index value increases with increasing HgS concentration especially at low wavelength. This type of high refractive indexed nanocomposites can be used in the wave guide technology, anti reflective coating, and photonic devices [35].

The dispersion plays a significant role in the research of optical materials, since it is an important factor in optical communication and in designing devices for spectral dispersion [36]. The Wemple and DiDomenico single oscillator model was used to analyses the dispersion of refractive index, which provides the useful parameters regarding the characterize the strength of inter-band transitions [37]. The dispersion of refractive index below the interband absorption edge according to the Wemple and DiDomenico single oscillator model [38] is given as:

$$n^2 = 1 + \frac{E_o E_d}{{E_o}^2 - (h\nu)^2} \qquad (4)$$

where E_o is the average values of single oscillator energy for electronic transitions, which usually been considered as an average energy gap, and E_d is the dispersion-energy, which is a measure of the average strength of inter-band optical transitions, and can be considered as a parameter having very close relation with the chemical bonding [38,39].

Table 1. The dispersion parameters and static refractive index of PVA/HgS nanocomposites films

HgS (M)	$E_o\ (eV)$	$E_d\ (eV)$	n_o
0	4.5245	0.9058	1.095536
0.01	4.1438	2.2983	1.246848
0.02	4.0936	2.5714	1.275986
0.03	4.0225	2.9952	1.320834
0.04	3.9414	4.3745	1.452542

The values of E_o and E_d were calculated directly from the slope $\left(-1/(E_o E_d)\right)$ and intercept (E_o/E_d) on the vertical axis of the linear fitted part of $1/(n^2-1)$ plot versus $(h\nu)^2$ (Figure 6). The obtained values of the E_o and E_d for the PVA/HgS nanocomposites are given in Table 1. Although E_d values increase with increasing HgS concentration, E_o values tend to decrease. The increase of dispersion energy E_d indicates the increase of bond strength, which lead to increases in degree of disorder. The oscillator energy E_o is related to the optical band gap E_g [24,40]. The E_o values of the present films is related empirically to the optical band gap by $E_o \approx 0.768E_g$.

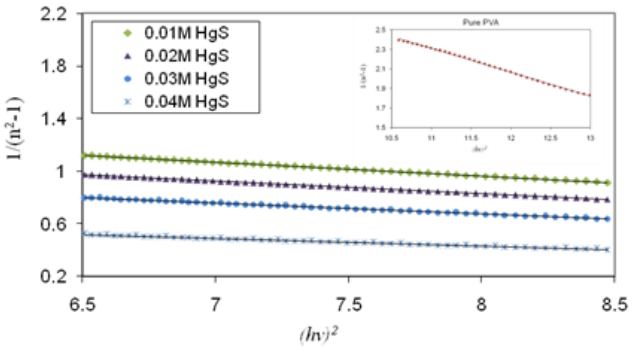

Figure 6. Plots of $1/(n^2-1)$ plot versus $(h\nu)^2$ of PVA/HgS nanocomposites

The static refractive index n_o at zero photon energy is evaluated from Eq. 6, i.e. $\left({n_o}^2 = 1 + \frac{E_d}{E_o}\right)$, the values are tabulated in Table 1. The static refractive index n_o of PVA/HgS nanocomposites increase with increasing HgS content.

Recently, it was reported that the linear behavior between n_o and the concentration of filler indicates the good or homogeneous dispersion of the filler inside the host polymer [29,41]. It can be seen from Figure 7 that the static refractive index n_o increased linearly with increasing the HgS concentration. The regression value is 0.932 as exhibited in Figure 7 and indicates almost a well fitting between the data points. This result was previously supported by the SEM images shown in Figure 2.

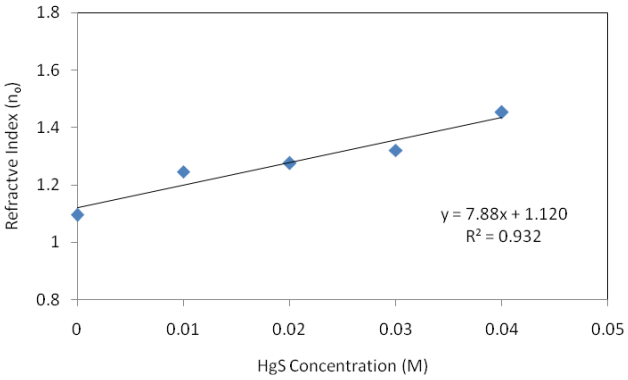

Figure 7. Static refractive index n_o as a function of HgS concentration

The dielectric constant (ε_r) and dielectric loss (ε_i) of the PVA/HgS nanocomposites samples are calculated from the relations [30]:

$$\varepsilon_r = n^2 - k^2; \varepsilon_i = 2nk \qquad (5)$$

The variation of dielectric constant (ε_r) and dielectric loss (ε_i) with wavelength for the PVA/HgS nanocomposite films having different concentrations of HgS nanoparticles are shown in Figure 8 and Figure 9. Both ε_r and ε_i values decrease with increasing wavelength,

and increase with increasing concentration of the HgS nanoparticle. The dielectric constant values ranged from 1.60 for pure PVA to 6.24 for 0.04M HgS composite at 300 nm wavelength. Thus, the results of this work indicate that a small amount of HgS nanoparticles can tune significantly the dielectric constant values.

The variation of ε_r and ε_i follow the same pattern, and it is seen that the values of ε_r are higher than values of ε_i. The dielectric constant ε_r relates to the dispersion, while the dielectric loss ε_i provides a measure of the dissipative rate of the wave in the medium.

The observed increase in the refractive index n, and dielectric constant ε_r due to the incorporation of nano filler content in the PVA matrix was reported in many researches [32,42].

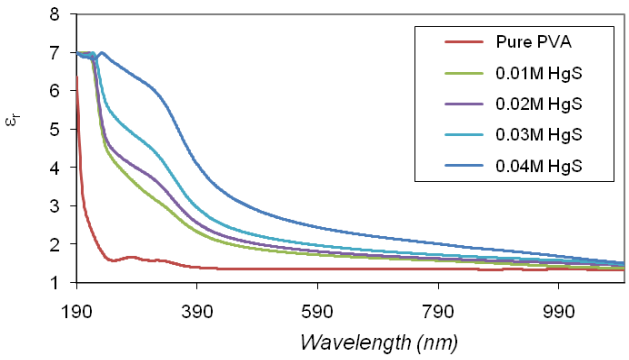

Figure 8. Dielectric constant (ε_r) versus wavelength of PVA/HgS nanocomposites

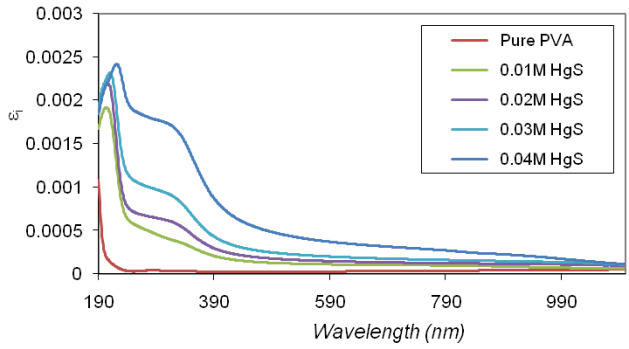

Figure 9. Dielectric loss (ε_i) versus wavelength of PVA/HgS nanocomposites

The relation between the optical dielectric constant ε_r and wavelength λ is given by the equation [34]

$$\varepsilon_r = \varepsilon_\infty - \frac{e^2}{4\pi^2 c^2 \varepsilon_o}\frac{N}{m^*}\lambda^2 \qquad (6)$$

where ε_∞ is the residual dielectric constant, e is the electronic charge, c is the light velocity, ε_o is the free space dielectric constant, and N/m^* ratio of carrier concentration to the effective mass. Figure 10 shows the relation between ε_r and λ^2 for the investigated nanocomposit samples. Extrapolating the lines of Figure 10 towards $\lambda^2 = 0$, the intercept at ε_r axis yields the value of ε_∞, which increases with increasing HgS content. From the slope, N/m^* can be estimated. The calculated values from Fig. 10 are given in Table 2.

It is clear that both ε_∞ and N/m^* values for PVA/HgS nanocomposite increase with increasing HgS content. This implies that with increasing concentration of HgS nanoparticles free carriers increase.

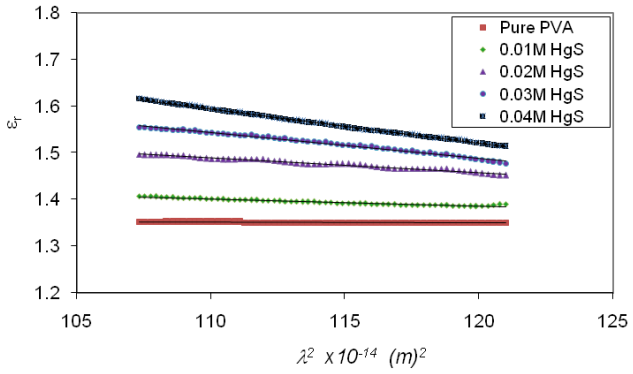

Figure 10. Plot of ε_r versus λ^2 for PVA/HgS nanocomposite films

Table 2. Values of optical parameters with respect to HgS nanoparticle content in PVA matrix.

HgS (M)	$N/m^*\ (m^{-3}Kg^{-1}) \times 10^{55}$	ε_∞
0	1.44687	1.364
0.01	19.7793	1.578
0.02	38.2679	1.831
0.03	68.4470	2.156
0.04	91.1028	2.409

According to these results, all optical parameters affected by HgS concentration, so the optical parameters of PVA films could be tuned by controlling the HgS concentration. The quantitative measurements of these parameters may help in adjusting and modeling the properties of such films for designing the optoelectronic devices.

3.5. Tuning Optical Band Gap

The control over the band gap is necessary while designing new materials for organic solar cells [43]. Reducing the band gap energy of polymer leads to development of new materials with maximum overlap of absorption spectrum with the solar emission spectrum.

The optical transitions occur when the energy of the absorbed photon is higher or equal to the forbidden energy band gap. If the incident photon energy is almost equal to the difference between the lowest level of the conduction band and the highest level of the valence band, some electrons from the valence band are able to jump across to the conduction band. At high absorption coefficient levels, where $\alpha > 10^4\ cm^{-1}$, the absorption coefficient α for noncrystalline materials can be related to the incident photon energy $(h\nu)$ according to the formula [7]:

$$\alpha h\nu = \beta\left(h\nu - E_g\right)^\gamma \qquad (7)$$

where β is a constant, E_g is the optical band gap, and the exponent γ is an index determined by the type of electronic transition causing the optical absorption and can take values 1/2, 3/2 for direct and 2, 3 for indirect transitions [32].

At lower absorption coefficient level $\alpha < 10^4\ cm^{-1}$, the value of $\alpha(\nu)$ is described by the Urbach formula [44]

$$\alpha(\nu) = \alpha_o \exp\left(\frac{h\nu}{E_u}\right) \qquad (8)$$

where α_o is a constant and E_u is the energy gap tail interpreted as the width of the tails of localized states in the forbidden band gap that associated with the amorphous nature of the materials [30].

Figure 11 shows graphs of $(\alpha hv)^2$ versus photon energy (hv) at room temperature. The obtained straight lines indicate that the electron transition is direct transition. Extrapolation of the linear portion of these curves gives the value of optical band gap (E_g).

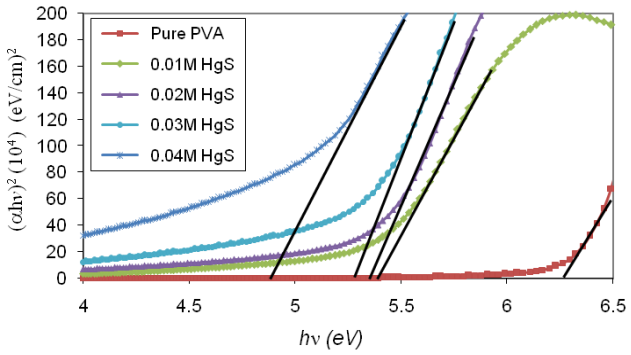

Figure 11. $(\alpha hv)^2$ versus photon energy (hv) for PVA/HgS nanocomposites.

Table 3 includes determined values of (E_g), which decrease with increasing HgS content from 6.27 eV for pure PVA to 4.88 eV for 0.04M HgS content.

Figure 12 presents the Urbach plots for the prepared nanocomposite films. The (E_u) values listed in Table 3 were determined from the slope reciprocal of the linear part of each curve.

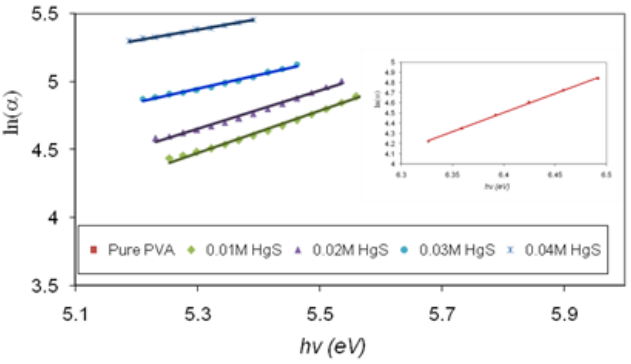

Figure 12. Urbach plot of $\ln(\alpha)$ versus photon energy (hv) for pure PVA and PVA/HgS nanocomposites films.

Table 3. Optical energy results for (HgS) composite films.

HgS (M)	$E_g\ (eV)$	$E_u\ (eV)$	α_o
0	6.27	0.26724	3.6084E-09
0.01	5.35	0.64475	0.02363563
0.02	5.27	0.70872	0.05919016
0.03	5.27	0.99701	0.69073433
0.04	4.88	1.26263	3.26741777

The exponential dependence of the absorption coefficient $\alpha(v)$ on photon energy (hv) indicates that the absorption processes obey the Urbach rule in the present samples. These energy tails widths increase as the concentration of HgS increases, which is consistent with the variation of the optical band gap (E_g). The increments of the energy tail widths can be explained by the fact that increasing the HgS content may lead to the creation of disorder, and imperfections in the structure of the composites, which lead to increase the localized states within the forbidden energy gap. This usually contributes to the decrease in the optical band gap [30,45].

4. Conclusion

In this work, polymer nanocomposite films of PVA/HgS have been prepared by in-situ chemical reduction, and casting techniques. FTIR studies confirmed the charge-transfer complex between PVA molecules and HgS nanoparticles. XRD analyzes revealed the formation of α-HgS crystal structure in the PVA film with an average diameter between (13.28 to 16.23) nm. Optical quantities such as absorption coefficient, refractive index, dielectric constants, optical band gap, and tails of localized states, were determined from analysis of the UV-Vis absorbance spectra. The direct optical band gap of nanocomposites decreases with increasing HgS content, whereas the observed dielectric constant and the refractive index increase with HgS content. The single oscillator model has been applied to analyze the dispersion of the refractive index of the prepared films.

Acknowledgement

The Authors are very much grateful to the University of Sulaimani, for providing financial assistance for this research. The authors gratefully acknowledge the Kurdistan Institution for Strategic Studies and Scientific Research, and the Ministry of Science and Technology for the facility in their laboratories.

References

[1] D.R. Paula, L.M. Robeson, "Polymer nanotechnology: Nanocomposites", Polymer, 49 (2008) 3187-3204.

[2] H.N. Chandrakala, B. Ramaraj, Shivakumaraiah, Siddara-maiah, "Optical properties and structural characteristics of zinc oxide cerium oxide doped polyvinyl alcohol films", Journal of Alloys and Compounds, 586 (2014) 333-342.

[3] S. Mahendia, A.K. Tomar, S. Kumar, "Nano-Ag doping induced changes in optical and electrical behaviour of PVA films", Mater. Sci. Eng., B 176 (2011) 530-534.

[4] P. Mulvaney, "Surface plasmon spectroscopy of nanosized metal particles", Langmuir 12 (1996) 788-800.

[5] S. Berciaud, L. Cognet, P. Tamarat, B. Lounis, "Observation of intrinsic size effects in the optical response of individual gold nanoparticles", Nano Lett. 5 (2005) 515-518.

[6] K.L. Kelly, E. Coronado, L.L. Zhao, G.C. Schatz, "The optical properties of metal nanoparticles: the influence of size, shape, and dielectric environment", J. Phys. Chem. B 107 (2003) 668-677.

[7] O.Gh. Abdullah, S.B. Aziz, K.M. Omer, Y.M. Salih, "Reducing the optical band gap of polyvinyl alcohol (PVA) based nanocomposite", J. Mater. Sci. Mater. Electron. 26 (2015) 5303-5309.

[8] O.Gh. Abdullah, D.A. Tahir, K. Kadir, "Optical and structural investigation of synthesized PVA/PbS nanocomposites", J. Mater. Sci. Mater. Electron. 26 (2015) 6939-6944.

[9] P. Chandra Sekhar, P. Naveen Kumar, U. Sasikala, V.V.R.N. Rao, A.K. Sharma, "Investigations on lithium ion complexed polyvinyl alcohol (PVA) solid polymer electrolyte films", IRACST-Engineering Science and Technology: An International Journal (ESTIJ), 2 (2012) 908-912.

[10] R.S. Al-Faleh, A.M. Zihlif, "A study on optical absorption and constants of doped poly(ethylene oxide)", Physica B: Condensed Matter 406 (2011) 1919-1925.

[11] D.Z. Qin, X.M. Ma, L. Yang, L. Zhang, Z.J. Ma, J.J. Zhang, "Biomimetic synthesis of HgS nanoparticles in the bovine serum albumin solution", J. Nanopart. Res. 10 (2008) 559-566.

[12] L. Zhang, G. Yang, G. He, L. Wang, Q. Liu, Q. Zhang, D. Qin, "Synthesis of HgS nanocrystals in the Lysozyme aqueous solution through biomimetic method", Applied Surface Science 258 (2012) 8185-8191.

[13] W. Wichiansee, M.N. Nordin, M. Green, R.J. Curry, "Synthesis and optical characterization of infra-red emitting mercury sulfide (HgS) quantum dots", J. Mater. Chem. 21 (2011) 7331-7336.

[14] T. Ren, S. Xu, W. Zhao, J. Zhu, "A surfactant-assisted photochemical route to single crystalline HgS nanotubes", J. Photochem. Photobio. A: Chem. 173 (2005) 93-98.

[15] P.S. Nair, T. Radhakrishnan, N. Revaprasadu, C.G.C.E. van Sittert, V. Djokovic, A.S. Luyt, "Characterization of polystyrene filled with HgS nanoparticles", Materials Letters 58 (2004) 361-364.

[16] P.S. Nair, T. Radhakrishnan, N. Revaprasadu, G.A. Kolawole, P. O'Brien, "The synthesis of HgS nanoparticles in polystyrene matrix", J. Mater. Chem. 14 (2004) 581-584.

[17] D. Qin, G. Yang, L. Zhang, X. Du, Y. Wang, "Synthesis and optical characteristics of PAM/HgS nanocomposites", Bull. Korean Chem. Soc. 35 (2014) 1077-1081.

[18] J.F. Zhu, Y.J. Zhu, M.G. Ma, L.X. Yang, L. Gao, "Simultaneous and rapid microwave synthesis of polyacrylamide-metal sulfide (Ag_2S, Cu_2S, HgS) nanocomposites", J. Phys. Chem. C, 111 (2007) 3920-3926.

[19] S. Wang, M. Zheng, "An easy approach to fabricating HgS/chitosan nanocomposite films and their ability to sense triethylamine", J. Polym. Eng. 34 (2014) 339-344.

[20] J.Z. Mbese, P.A. Ajibade, "Preparation and characterization of ZnS, CdS and HgS/Poly(methyl methacrylate) nanocomposites polymers, 6 (2014) 2332-2344.

[21] K.S. Hemalatha, K. Rukmani, N. Suriyamurthy, B.M. Nagabhushana, "Synthesis, characterization and optical properties of hybrid PVA-ZnO nanocomposite: A composition dependent study", Materials Research Bulletin 51 (2014) 438-446.

[22] J. Xu, X. Cui, J. Zhang, H. Liang, H. Wang, J. Li, "Preparation of CuS nanoparticles embedded in poly(vinyl alcohol) nanofibre via electrospinning", Bull. Mater. Sci. 31 (2008) 189-192.

[23] X. Yuan, "Enhanced interfacial interaction for effective reinforcement of poly(vinyl alcohol) nanocomposites at low loading of graphene", Polym. Bull. 67 (2011) 1785-1797.

[24] R.P. Chahal, S. Mahendia, A.K. Tomar, S. Kumar, "γ-Irradiated PVA/Ag nanocomposite films: Materials for optical applications", Journal of Alloys and Compounds 538 (2012) 212-219.

[25] S. Sarma, P. Datta, "Characteristics of poly(vinyl alcohol)/lead sulphide quantum dot device", Nanoscience and Nanotechnology Letters 2 (2010) 261-265.

[26] S. Wu, C. Chen, X. Shen, G. Li, L. Gao, A. Chen, J. Hou, X. Liang, "One-pot synthesis, formation mechanism and near-infrared fluorescent properties of hollow and porous α-mercury sulfide", Cryst. Eng. Comm. 15 (2013) 4162-4166.

[27] R. Selvaraj, K. Qi, S.M.Z. Al-Kindy, M. Sillanpaa, Y. Kim, C.W. Tai, "A simple hydrothermal route for the preparation of HgS nanoparticles and their photocatalytic activities", RSC Adv. 4 (2014) 15371-15376.

[28] M. Sharma, S.K. Tripathi, "Photoluminescence study of CdSe nanorods embedded in a PVA matrix", Journal of Luminescence 135 (2013) 327-334.

[29] F.F. Muhammad, S.B. Aziz, S.A. Hussein, "Effect of the dopant salt on the optical parameters of PVA:NaNO3 solid polymer electrolyte", J. Mater. Sci. Mater. Electron. 26 (2015) 521-529.

[30] S. Elliot, The Physics and Chemistry of Solids, John Wiley & Sons, New York, (1998).

[31] E.A. Davis, N.F. Mott, "Conduction in non-crystalline systems V. Conductivity, optical absorption and photoconductivity in amorphous semiconductors", Philos. Mag. 22 (1970) 903-922.

[32] O.Gh. Abdullah, D.R. Saber, L.O. Hamasalih, "Complexion formation in PVA/PEO/$CuCl_2$ solid polymer electrolyte", Universal Journal of Materials Science, 3 (2015) 1-5.

[33] A.A. Jamous, A.M. Zihlif, "Study of the electrical conduction in poly(ethylene oxide) doped with iodine", Physica B: Condensed Matter 405 (2010) 2762-2767.

[34] F. Yakuphanoglu, H. Erten, "Refractive index dispersion and analysis of the optical constants of an ionomer thin film", Optica Applicata 35 (2005) 969-976.

[35] A.N. Alias, Z.M. Zabidi, A.M.M. Ali, M.K. Harun, M.Z.A. Yahya, "Optical characterization and properties of polymeric materials for optoelectronic and photonic applications", International Journal of Applied Science and Technology, 3 (2013) 11-38.

[36] Z.M. Elimat, A.M. Zihlif, G. Ragosta, "Optical characterization of poly (ethylene oxide)/alumina composites", Physica B: Physics of Condensed Matter 405 (2010) 3756-3760.

[37] M.P. Moret, M.A.C. Devillers, K. Worhoff, P.K. Larsen, "Optical properties of $PbTiO_3$, $PbZr_xTi_{1-x}O_3$, and $PbZrO_3$ films deposited by metalorganic chemical vapor on $SrTiO_3$", Journal of Applied Physics 92 (2002) 468-474.

[38] S.H. Wemple, M. DiDomenico, "Behavior of the electronic dielectric constant in covalent and ionic materials", Phys. Rev. B3 (1971) 1338-1351.

[39] I. Saini, J. Rozra, N. Chandak, S. Aggarwal, P.K. Sharma, A. Sharma, "Tailoring of electrical, optical and structural properties of PVA by addition of Ag nanoparticles", Materials Chemistry and Physics 139 (2013) 802-810.

[40] A. Benchaabane, Z.B. Hamed, F. Kouki, M.A. Sanhoury, K. Zellama, A. Zeinert, H. Bouchriha, "Performances of effective medium model in interpreting optical properties of polyvinylcarbazole:ZnSe nanocomposites", Journal of Applied Physics 115 (2014) 134313.

[41] S.B. Aziz, H.M. Ahmed, A.M. Hussein, A.B. Fathulla, R.M. Wsw, R.T. Hussein, "Tuning the absorption of ultraviolet spectra and optical parameters of aluminum doped PVA based solid polymer composites", J. Mater. Sci. Mater. Electron. 26 (2015) 8022-8028.

[42] S. Sugumaran, C.S. Bellan, "Transparent nano composite PVA–TiO_2 and PMMA–TiO_2 thin films: Optical and dielectric properties", Optik 125 (2014) 5128-5133.

[43] C. Kanimozhi, P. Balraju, G.D. Sharma, S. Patil, "Synthesis of diketopyrrolopyrrole containing copolymers: A study of their optical and photovoltaic properties", J. Phys. Chem. B 114 (2010) 3095-3103.

[44] F. Urbach, "The long-wavelength edge of photographic sensitivity and of the electronic absorption of solids", Phys. Rev. 92 (1953) 1324.

[45] S.A. Sbeih, A.M. Zihlif, "Optical and electrical properties of kaolinite/ polystyrene composite", J. Phys. D: Applied Physics 24 (2009) 145405.